Final Report for AOARD Grant 104087

"Smart Nanofibers Self-Assembled from Dumbbell-Shaped Rod Amphiphiles"

20110901

Name of Principal Investigator(s): Myongsoo Lee
- e-mail address: myongslee@snu.ac.kr
- Institution: Seoul National University
- Department: Chemistry
- Mailing Address: Seoul National university, Department of Chemistry, Seoul, 151-747-Republic of Korea
- Phone: 82-2-880-4340
- Fax: 82-2-393-6096

Period of Performance: 04/12/2010 – 04/11/2011

Abstract: **A carbazole end-capped rod amphiphile was synthesized and observed to self-assemble into non-chiral fibers in both methanol and water solutions even though the molecule contains chiral oligoether side groups. Remarkably, a mixture solution of water and methanol induces supramolecular chirality of the nanofibers caused by conformational change of hydrophobic aromatic rods and reduction in hydrodynamic volume of ethylene oxide. The helicity induction of the nanofibers also takes place by heating the water solution. Furthermore, the helical fibers in aqueous solution were observed further aggregate into a rigid gel at higher temperature by enhanced hydrophobic interactions between oligo(ethylene oxide) dendrons.**

Introduction: The construction of novel functional materials based on molecular self-assembly has received a great deal of attention in the fields of molecular and supramolecular materials. Among the supramolecular nanostructures formed by the self-assembly of specifically designed molecules, a one-dimensional (1D) fibrillar assembly has proved to be particularly interesting for applications such as nanowires, gels, and biomemetic systems. The 1D structures with stimulus-responsive features is likely to be further enhance their scope as smart nanoscale materials. Although stimulus-responsive 1D nanostructures have been extensively studied, switching behavior triggered by external stimuli with 1D fibrillar objects remains challenging. We have shown that discrete cylindrical micelles can be interconnected by addition of a bridging agent to form reversible gels in aqueous solution. We have also shown that T-shaped aromatic amphiphiles self-assemble into thermoresponsive nanofibers to form a 3D network gel upon heating.

Recently, we have demonstrated that achiral nanofibrers formed from dumbbell-shaped rod amphiphile based on oligoether dendrons undergo a transition into chiral helical fibers triggered by lower critical solution temperature (LCST) of external oligoether chains in aqueous solution. We envisioned that the amphiphilc molecules based on a conjugated rod can self-assemble into nanostructures even in polar organic solvents such as methanol, which is a selective solvent for oligoether dendrons. With this idea in mind, we prepared amphiphile **1** containing a carbazole end-capped hexa-*p*-phenylene as a aromatic rod and oligo(ethylene oxide) dendrons according to previously reported similar methods and characterized by ^{1}H NMR spectroscopy and MALDI-TOF mass spectrometry. We present herein the formation of stimulus-responsive nanofibers from the self-assembly of rod amphiphiles. Notably, the self-assembled nanofibers respond to external stimuli such as

1. REPORT DATE **30 SEP 2011**	2. REPORT TYPE **Final**	3. DATES COVERED **13-04-2010 to 13-04-2011**
4. TITLE AND SUBTITLE **Smart Nanofibers Self-Assembled from Dumbbell-Shaped Rod Amphiphiles**		5a. CONTRACT NUMBER **FA23861014087**
		5b. GRANT NUMBER
		5c. PROGRAM ELEMENT NUMBER
6. AUTHOR(S) **Myong Soo Lee**		5d. PROJECT NUMBER
		5e. TASK NUMBER
		5f. WORK UNIT NUMBER
7. PERFORMING ORGANIZATION NAME(S) AND ADDRESS(ES) **Seoul National University,Seoul,Seoul 151-747,Korea,NA,NA**		8. PERFORMING ORGANIZATION REPORT NUMBER **N/A**
9. SPONSORING/MONITORING AGENCY NAME(S) AND ADDRESS(ES) **AOARD, UNIT 45002, APO, AP, 96338-5002**		10. SPONSOR/MONITOR'S ACRONYM(S) **AOARD**
		11. SPONSOR/MONITOR'S REPORT NUMBER(S) **AOARD-104087**
12. DISTRIBUTION/AVAILABILITY STATEMENT **Approved for public release; distribution unlimited**		
13. SUPPLEMENTARY NOTES		

14. ABSTRACT

This report covers efforts directed toward self assembly of rod-coil block molecules for use as smart nanofibers. A carbazole end-capped rod amphiphile was synthesized and observed to self-assemble into non-chiral fibers in both methanol and water solutions even though the molecule contains chiral oligoether side groups. A mixture solution of water and methanol induces supramolecular chirality of the nanofibers caused by conformational change of hydrophobic aromatic rods and reduction in hydrodynamic volume of ethylene oxide. The helicity induction of the nanofibers also takes place by heating the water solution. Furthermore, the helical fibers in aqueous solution were observed further aggregate into a rigid gel at higher temperature by enhanced hydrophobic interactions between oligo(ethylene oxide) dendrons.

15. SUBJECT TERMS					
nano devices , smart nanofibers					

16. SECURITY CLASSIFICATION OF:			17. LIMITATION OF ABSTRACT	18. NUMBER OF PAGES	19a. NAME OF RESPONSIBLE PERSON
a. REPORT **unclassified**	b. ABSTRACT **unclassified**	c. THIS PAGE **unclassified**	**Same as Report (SAR)**	**7**	

temperature and solvent polarlity by chiral induction.
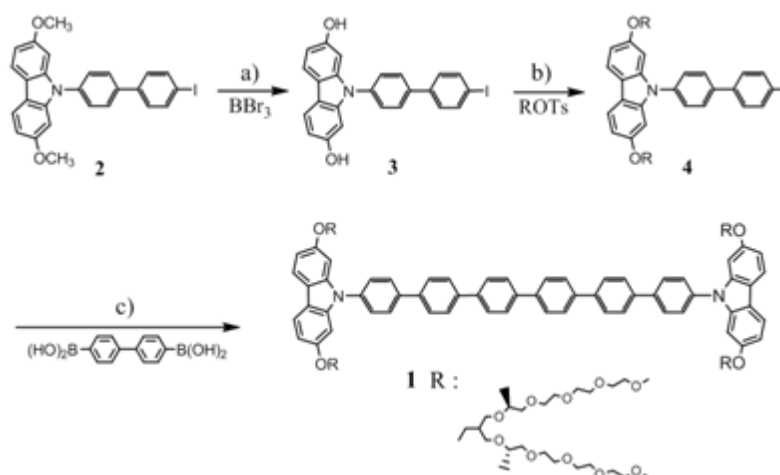
Scheme 1. Synthesis of the end-capped rod amphiphile 1. a) dichloromethane; b) K_2CO_3, acetonitrile, reflux; c) Na_2CO_3, $[Pd(PPh_3)_4]$, THF, reflux.

Experiment: Materials

NaH (60%), and *p*-toluenesulfonyl chloride (98%) from Tokyo Kasei 4,4'-diiodobiphenyl (98%) from Lancaster were used as received. ethyl-(s)-lactate and unless otherwise indicated, all starting materials were obtained from commercial suppliers from Aldrich were used without purification. Dry THF was obtained by vacuum transfer from sodium and benzophenone. Compounds were synthesized according to the procedure described scheme 1 and the synthesis of staring materials **2** and oligo-ethylene oxide segments were synthesized using a similar procedure described previously.

Techniques

^{1}H-NMR spectra were recorded from $CDCl_3$ or DMSO solutions on a Bruker AM 250 spectrometer. Dynamic light scattering (DLS) measurements were performed using DLS-8000 from Otsuka Electronics with a 632.8 nm He-Ne laser. UV/vis absorption spectra were obtained from a Hitachi U-2900 Spectrophotometer. The fluorescence spectra were obtained from a Hitachi F-7000 Fluorescence Spectrophotometer. Circular dichroism (CD) spectra were obtained using JASCO J-810 spectropolarimeter. Transmission electron microscope (TEM) was performed at 120 kV using JEOL-JEM 2100. MALDI-TOF-MS was performed on a Bruker Microflex LRF20 using α-cyano-4-hydroxy cinnamic acid (CHCA) as matrix. Preparative high performance liquid chromatography (HPLC) was performed at room temperature using a 20 mm x 600 mm poly styrene column on a Japan Analytical Industry Model LC-908 recycling preparative HPLC system, equipped with UV detector 310 and RI detector RI-5.

Synthesis

Synthesis of compound 3: Droping BBr_3 (15ml, 15mmol) to a solution of compound **2** (1.24 g, 2.45 mmol) in methylene chloride 40mL slowly at 0 °C. The reaction mixture was stirred at room temperature under nitrogen for 6 h. The solution was quenched with MeOH for 30 min. Then the resulting solution was washed with water and the methylene chloride solution dried over anhydrousmagnesium sulfate, and filtered. The solvent was removed in a rotary evaporator, and the crude product was purified by column chromatography (silica gel) using ethyl acetate: hexane (2:3 v/v) to yield 1.1 g (94%) of a white powder. ^{1}H-NMR (250 MHz, DMSO, δ, ppm) 9.36 (s, 2H, ArOH), 7.89 (m, 6Ar-H), 7.6 (m, 4Ar-H) 6.69 (m, 4 Ar-H).

Synthesis of compound 4: Compound **3** (0.23 g, 0.47 mmol), ROTs (0.72 g, 1.08 mmol) and excess K_2CO_3 were dissolved in 30 ml of anhydrous acetonitrile. The mixture was refluxed for 24 h. The resulting solution was poured into water and extracted with methylene chloride.

The methylene chloride solution was washed with water, dried over anhydrous magnesium sulfate, and filtered. The solvent was removed in a rotary evaporator, and the crude product was purified by column chromatography (silica gel) using ethyl acetate/ methanol (20:1 v/v) to yield 0.58 g (68 %) of a waxy solid. ^{1}H-NMR (250 MHz, CDCl$_3$, δ, ppm) 7.87 (d, 2Ar-H, o to I, 8.8 Hz), 7.77 (m, 4Ar-H), 7.59 (d, 2Ar-H, m to OCH2, 8.5 Hz), 7.44 (d, 2Ar-H, m to I, 8.8Hz), 6.85 (m, 4Ar-H), 4.11 (d, 4H, 2× CH_2Ophenyl, J = 3.5 Hz), 3.82-3.51 (m, 68H, OCH_2), 3.37 (s, 12H, OCH_3), 2.2-2.5 (m, 2H, 2×CH(CH$_2$)$_3$), 1.06–1.17 (m, 12H, 4×CHCH_3).

*Synthesis of compound **1**:* Compound **4** (0.36 g, 0.239 mmol) and 4,4'-biphenyl diboronic acid (28.8 mg, 0.12 mmol) were dissolved in degassed THF (25 ml). Degassed 2 M aqueous Na$_2$CO$_3$ (25 ml) was added to the solution and then tetrakis (triphenylphosphine) palladium(0) (5 mg, 0.004 mmol) was added. The mixture was refluxed for 24 h with vigorous stirring under nitrogen. Cooled to room temperature, the layers were separated, and the aqueous layer was then washed twice with methylene chloride. The combined organic layer was dried over anhydrous magnesium sulfate and filtered. The solvent was removed in a rotary evaporator, and the crude product was purified by column chromatography (silica gel) using ethyl acetate/ methanol (10:1 v/v) as eluent and by prep. HPLC to yield 0.14 g (40 %) of a waxy solid. ^{1}H-NMR (250 MHz, CDCl$_3$, δ, ppm) 7.93-7.81 (m, 24Ar-H), 7.65 (d, 4Ar-H, m to OCH$_2$, 8.5 Hz), 6.86 (m, 8Ar-H), 4.06 (d, 8H, 4× CH_2Ophenyl, J = 4.8 Hz), 3.64-3.49 (m, 136H, OCH_2), 3.36 (m, 24H, OCH_3), 2.37-2.31 (m, 4H, phenylOCH$_2$$CH$(CH$_2$O)$_2$), 1.13–1.08 (m, 24H, 8×CHCH_3): ^{13}C-NMR (60 MHz, CDCl$_3$, ppm) : = 157.9, 142.2, 139.9, 139.8, 139.6, 137.0, 128.7, 127.7, 127.6, 119.0, 117.2, 95.2, 71.7, 70.8, 70.5, 69.7, 69.4, 66.5, 59.1, 40.2, 17.43, 17.30; Anal. Calcd for C$_{156}$H$_{232}$N$_2$O$_{44}$: C, 65.99; H, 8.24; N, 0.99. Found C, 65.65; H, 8.32; N, 1.03. MALDI-TOF-MS m/z (M+H)$^+$ 2840.5, (M+Na)$^+$ 2862.8.
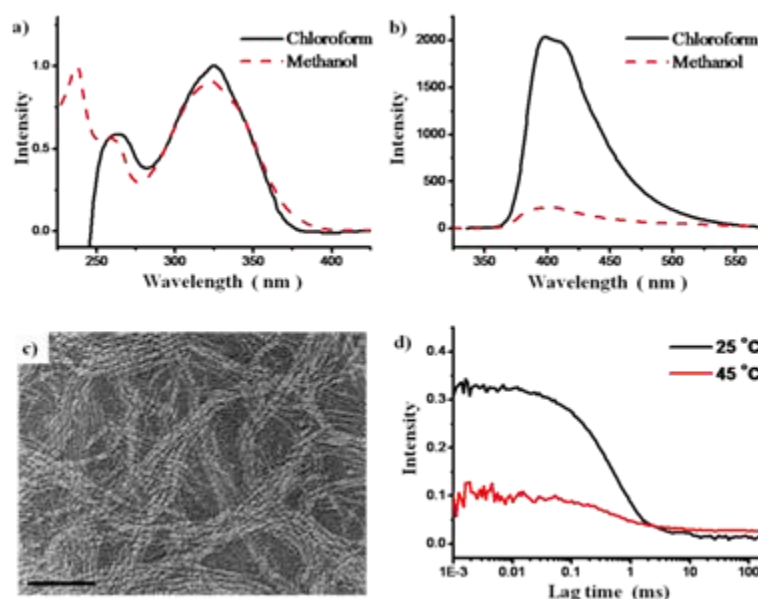
Results and Discussion:

Fig. 1 a) Absorption spectra of **1** in chloroform (2.0×10^{-5} M, black), methanol (2.0×10^{-5} M, red). b) Emission spectra of **1** in chloroform (2×10^{-5} M, black), methanol (2×10^{-5} M, red). c) TEM images of **1** methanol solution prepared at 25 ^{o}C (4×10^{-4} M, scale bars: 50 nm). d) Autocorrelation functions of **1** in methanol (4×10^{-4} M) at 25 ^{o}C(black) and at 45 ^{o}C(red).

The molecule **1**, when dissolved in a solvent suitable for the oligoether dendron, can

self-assemble into an aggregation structure due to their amphiphilic characteristics. Subsequently, the aggregation behavior of **1** in methanol was studied using UV/Vis and fluorescence spectroscopy. The solution of **1** in chloroform (2.0 × 10⁻⁵ M) shows an absorption maximum at 325 nm (п-п* transition) and emission maxima at λ = 397 and 410 nm (Fig. 1). Such spectra are similar to a general feature of 9-arylcarbazole derivatives revealing that there is a non-zero dihedral angle between the carbazole and hexa-*p*-phenylene unit. On the contrary, the maximum of absorption is blue-shifted with respect to that observed in chloroform, and fluorescence is significantly quenched, indicative of strong H-type interactions between the aromatic segments (Fig. 1). Dynamic light scattering (DLS) experiments were performed with **1** in methanol solution (4.0 × 10⁻⁴ M) to further investigate the aggregation behavior. The CONTIN analysis of the autocorrelation function of **1** shows a broad peak that corresponds to a hydrodynamic radius (R_H) of ~ 100 nm. To confirm the aggregation structures in methanol solution, the TEM experiments were performed. As shown in Figure 1c, the TEM image of **1** with a negatively stained sample shows one dimensional cylindrical fibers with a uniform diameter of about 4.8 nm and lengths of several micrometers. Considering the extended molecular length (5.3 nm by CPK modeling), the image indicates that the diameter of the elementary cylindrical objects corresponds to one molecular length. This result suggests that molecule **1** self-assembles into cylindrical micelles consisting of solvophobic aromatic segments surrounded by solvophilic dendritic segments that are exposed to the methanol environment. Within the core, the rod segments stack on top of each other with mutual rotations to reduce steric repulsions between the twisted, non-planar aromatic rods. Notably, when the molecule **1** in methanol solution was subjected to circular dichroism (CD) measurements, no CD signals could be detected even though **1** contains chiral side groups, indicating that the fibrillar objects are nonchiral. A temperature-dependent experiment reveals also no CD signal on heating and DLS shows that molecule **1** are molecularly dissolved over 45 °C (Fig. 1d). These results imply that the rod segment would be loosely packed with random stacks in methanol solution due to a non-planar aromatic conformation.
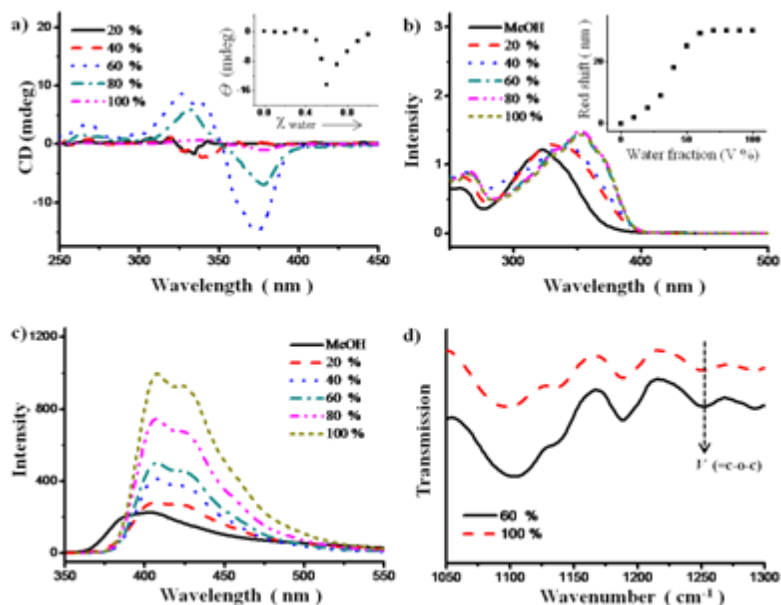

Fig. 2 a) CD spectra of **1** in mixed solution with 10 mm cell (2 × 10⁻⁵ M); The inset shows the CD intensity variation at 378 nm with increasing mole fraction of water. b) Absorption spectra of **1** in mixed solution (2.0 × 10⁻⁵ M); Inset shows the changes in the absorption maximum peak of **1**. c) Emission spectra of **1** in chloroform (2 × 10⁻⁵ M). d) FTIR spectra (1050 ~ 1300 cm⁻¹) of **1** in mixed solution (water : 60%, black) and aqueous solution

(red).

To investigate the influence of water on the methanol solution, the aggregation behavior was studied by addition of water into methanol solution (2×10^{-5} M). Remarkably, the CD spectra showed a strong positive and negative Cotton effect as the 60 % water addition accompanied by notable changes in the absorption and emission spectra (Fig. 2a), indicating that the formation of helical stacks of the rod segments with a preferred handeness. Upon addition of water into methanol solution of **1**, the absorption was red shifted and the intensity of emission was increased, indicating that effective conjugation length of aromatic rod is extended due to the transition from twisted to planar conformations (Fig. 2b). However, further addition of water results in a decrease in the intensity of the CD signal, which eventually disappeared in pure water. On the other hand, gradual increase of emission intensity was observed, suggesting the distance between the adjacent rods within the fibers increases due to increasing effective volume fraction of oligoether dendrons caused by hydrogen bonding between ether oxygens and water molecules. The hydrated feature is reflected in FTIR spectroscopic experiments (Fig. 2d). The IR of **1** in mixed solution of methanol-water (2 : 3) showed two characteristic bands at 1250 cm^{-1} and 1105 cm^{-1}, which corresponding to phenyl ring-O and aliphatic C-O stretchings. The band of 1105 cm^{-1} shifted to 1097 cm^{-1}, indicating that the hydrophilic oligoether chains are hydrated with addition of water through a hydrogen bonding interaction. This unique feature of the induction of the chirality can be explained by a conformational change of hydrophobic aromatic rods and variation in hydrodynamic volumes. Addition of water into the methanol solution would strengthen hydrophobic and π-π stacking interactions, which drives rod segments to be more planar for closer packing to result in steric constraints, giving rise to a helical arrangement. Further addition of water solvent, however, the oligoether chains would by fully hydrated to increase effective volume fraction of oligoether chains. This increment would frustrate π-π stacking of aromatic rods which allow the rod segments to freely rotate within the aromatic core to block the chiral transfer from the side groups to the aromatic cores, thereby leading to non-chiral fibers (Fig. 3).
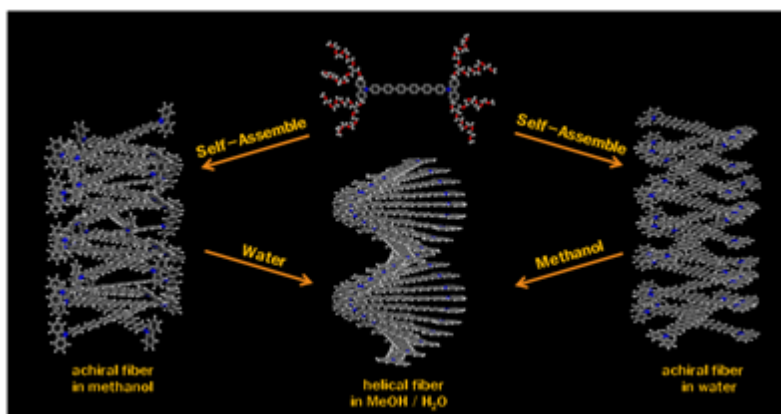

Fig. 3 Schematic representation of the reversible transformation from achiral to chiral states of the cylindrical stack in mixture of methanol and water.

The nanofibers formed in aqueous solution would be entangled with each other above a LCST transition due to enhanced hydrophobic interactions. In this context, we have measured viscosities with a capillary viscometer as a function of temperature. The solution viscosity of **1** (1.6×10^{-3} M) increases abruptly above 29 ^{o}C and results in gelation at 40 ^{o}C. This transition temperautre decreases to 10 ^{o}C with increasing concentration up to 1.4×10^{-2} M (Fig. 4a). The TEM image of the gel dried on a carbon-coated copper grid revealed the

formation of bundles of the nanofibes at higher temperatures, which demonstrates that the gel formation is attributed to the interconnection of the randomly oriented nanofibers (Fig. 4b). Interestingly, the CD spectra of **1** (1.6×10^{-3} M) showed a strong Cotton effect above the transition temperature, indicating the formation of helical stacks of the rod segments with a preferred handedness (Fig. 4c). Upon heating, the absorption spectra showed reduced intensity and the fluorescence was quenched, indicating that the π-π stacking interactions between the aromatic rods are enhanced (Fig. 4d). These results suggest that the helicity induction of the nanofibers upon heating arises from closer packing between the adjacent aromatic units within the core and the helical fibers were further aggregated into a rigid gel above a certain concentration. This thermoresponsive solution behavior can be explained by considering the entropically-driven dehydration of the oligoether chains, as the solution is heated. With increasing temperature, the ethylene oxide chains would be dehydrated that drives the fibers with more hydrophobic surfaces, thus resulting in enhanced hydrophobic interactions between the adjacent fibrils to form 3D networks. This enhanced hydrophobic environment also leads to a decrement of aromatic stacking distance with restricted rotational freedom thus the helical stacks are formed through steric constraints of the aromatic segments.
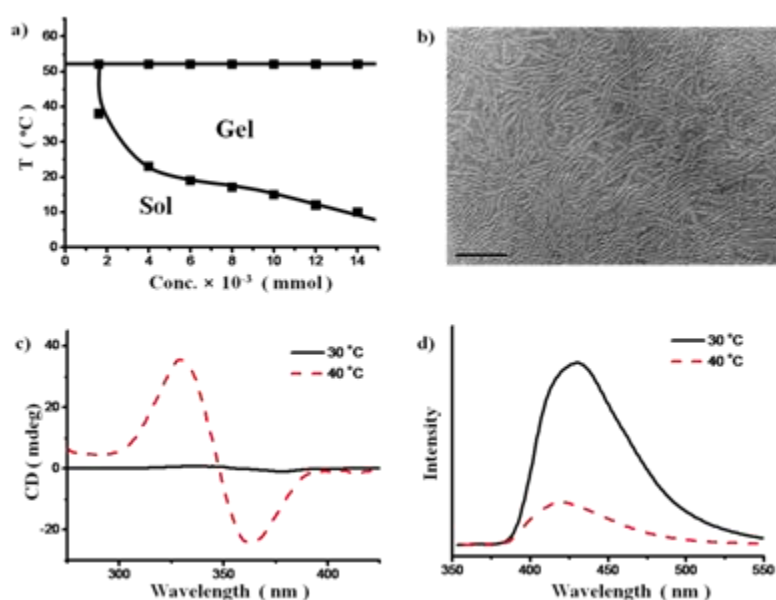

Fig. 4 a) Phase diagram plotted in terms of the concentration of **1** versus temperature. b) TEM images (negatively stained with uranyl acetate) of **1** in aqueous solution prepared at 40 ^{o}C (1.6×10^{-3} M, scale bars: 100 nm). c) CD spectra of **1** in aqueous solution with 1 mm cell (1.6×10^{-3} M). d) Emission spectra of **1** in aqueous solution (1×10^{-3} M) at 30 ^{o}C (black) and 40 ^{o}C (red).

List of Publications and Significant Collaborations:
a) Z. Huang, S.-K. Kang, M. Lee, Induction of Supramolecular Chirality in Self-Assembled Nanofibers Triggered by Environmental Change. *J. Mater. Chem*. **DOI:10. 1039/C1JM12683K**

DD882: As a separate document, please complete and sign the inventions disclosure form.

This document may be as long or as short as needed to give a fair account of the work

performed during the period of performance. There will be variations depending on the scope of the work. As such, there is no length or formatting constraints for the final report. Keep in mind the amount of funding you received relative to the amount of effort you put into the report. For example, do not submit a $300k report for $50k worth of funding; likewise, do not submit a $50k report for $300k worth of funding. Include as many charts and figures as required to explain the work. A final report submission very similar to a full length journal article will be sufficient in most cases.